Supplementary Information

Core-shell potassium niobate nanowires for enhanced nonlinear optical effects

J. Richter[a], A. Steinbrück[a], M. Zilk[a], A. Sergeyev[a], T. Pertsch[a], A. Tünnermann[a,b] and R. Grange[*,a]

[a] Institute of Applied Physics, Friedrich-Schiller-Universität Jena, Albert-Einstein Straße 15, 07745 Jena, Germany

[b] Fraunhofer Institute of Applied Optics and Precision Engineering, Albert Einstein Straße7, 07745 Jena, Germany

[*] *E-mail:* rachel.grange@uni-jena.de

1. Protocol for the shell growth synthesis

Silanization process

In a first step we immersed the wires in acid to take off surface potassium. After three centrifugation/water wash cycles the wires were redistributed in H_2O. A 1000:1:10 ratio of H_2O, acidic acid and (Aminopropyl)triethoxysilane was mixed and left to react for 5 minutes. After adding the nanowires we let the mixture react for another few minutes before washing and resuspending the aminosilane coated wires in H_2O. For positive charging of the outer layer of AMPTS, acid was added.

Adaption of Caruso process for functionalization

As an alternative method to explore the formation of gold shells we used Poly(diallyldimethylammonium chloride) (PDADMAC) obtained from Aldrich. A single layer polyelectrolyte film of PDADMAC was deposited on the $KNbO_3$ nanowires. A volume of 0.5 ml of a 1 mg/ml aqueous solution containing 0.5 M NaCl was added to 0,5 ml of nanowires dispersed in H_2O. The dispersion was stirred for 20 min to allow homogeneuos adsorption on the wires. The excess polyelectrolyte was removed by repeated centifugation/wash cycles.

Attachment of gold seeds to nanowires and shell growth

Between 3 ml and 5 ml of the gold seed solution was added to 0.1 µl to 0.3µl of aqueous nanowire dispersion. In the case of the aminosilane coated wires hydrochloric acid has to be added first to adjust the pH to 3.5 in order to get a positively charged surface. We let the mixture react for a maximum of four hours and washed the product by repeated centrifugation/water redispersion cycles. The sediment after the seeding usually showed a dark color while the redispersed solution is slightly pinkish.

To obtain a stable $Au(OH)_3$ solution, we added 5 ml of a 23 mM K_2CO_3 aqueous solution to 1.25 ml of a 12.5 mM $HAuCl_4$ solution and let it react for up to two days in the dark.

Finally, for the shell growth an amount of 400 µl of the seeded nanowires is diluted with 3 ml H_2O. 1 ml of the aged K-gold solution is added. To start the growth of the gold shell around the seeds on the wires 20 mmol hydroxylamine solution is added as a reducing agent. The reaction takes place immediately and results in a clear pink solution. Stabilisation of the particles in solution was achieved by adding sodium citrate.

2. Calculation of the optical response of core-shell nanowires

The linear optical response of the core-shell nanowires can be solved analytically. Therefore we divide the scattering geometry into three domains (Fig. S1): The nanowire core with radius $R_1 = r_c$ and refractive index $n_1 = \sqrt{\varepsilon_c}$, the nanowire shell with an outer radius $R_2 = r_s$ and refractive index $n_2 = \sqrt{\varepsilon_s}$ and the exterior with refractive index n_3. In each domain l the electric and the magnetic fields are expanded into cylindrical harmonics [1–3]:

$$\begin{aligned}\mathbf{E}_l &= \sum_{m=-\infty}^{\infty} \left(\imath a_{lm}\mathbf{m}_{lm} + b_{lm}\mathbf{n}_{lm} + \imath A_{lm}\mathbf{M}_{lm} + B_{lm}\mathbf{N}_{lm}\right) \text{ and} \\ \mathbf{H}_l &= \frac{n_l}{\imath Z_0}\sum_{m=-\infty}^{\infty} \left(\imath a_{lm}\mathbf{n}_{lm} + b_{lm}\mathbf{m}_{lm} + \imath A_{lm}\mathbf{N}_{lm} + B_{lm}\mathbf{M}_{lm}\right)\end{aligned} \tag{1}$$

whereby Z_0 denotes the free space impedance.

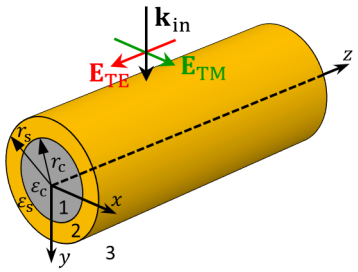

Figure S1: Considered geometry of the core-shell nanowire.

If we restrict the problem to the case of propagation normal to the nanowire axis, the vector-cylindrical harmonics in polar coordinates (r, ϕ) are given are given by

$$\begin{aligned}\mathbf{m}_{lm} &= \left[\frac{\imath m}{k_l r}H_m(k_l r)\mathbf{e}_r - H'_m(k_l r)\mathbf{e}_\phi\right]e^{\imath m\phi}, \\ \mathbf{n}_{lm} &= H_m(k_l r)\mathbf{e}_z e^{\imath m\phi}, \\ \mathbf{M}_{lm} &= \left[\frac{\imath m}{k_l r}J_m(k_l r)\mathbf{e}_r - J'_m(k_l r)\mathbf{e}_\phi\right]e^{\imath m\phi} \text{ and} \\ \mathbf{N}_{lm} &= J_m(k_l r)\mathbf{e}_z e^{\imath m\phi}.\end{aligned} \tag{2}$$

Thereby J_m is the Bessel function of the order m and H_m is the Hankel function of the first kind of the order m. The dash indicates the derivative with respect to the argument. $k_l = 2\pi n_l/\lambda$ is the magnitude of the wave vector in the domain l with the refractive index n_l and the free space wavelength λ. From the definition of the cylindrical harmonics it is obvious that for TM polarization $b_{lm} = B_{lm} = 0$ and for TE polarization $a_{lm} = A_{lm} = 0$ (the polarization directions are given in Fig. S1). The exciting wave is given by the coefficients $A_{3,m}$ and $B_{3,m}$. The coefficients $a_{1,m}$ and $b_{1,m}$ are nonzero only if source multipoles are present in the core. Otherwise they have to vanish due to the singularity of the Hankel functions at the origin. The remaining unknown coefficients can be determined by matching the tangential fields at the boundaries of the layers of the nanowire and solving the resulting system of linear equations. After some lengthy calculations one obtains for TM polarization

$$\begin{aligned} A_{1,m} &= \frac{-A_{3,m}\epsilon\kappa + a_{1,m}(\gamma\nu + \delta\sigma)}{\alpha\delta - \beta\gamma}, a_{2,m} = \frac{A_{3,m}\beta\kappa - a_1\delta\lambda}{\alpha\delta - \beta\gamma}, \\ A_{2,m} &= \frac{-A_{3,m}\alpha\kappa + a_{1,m}\gamma\lambda}{\alpha\delta - \beta\gamma}, \text{ and } a_{3,m} = -\frac{A_{3,m}(\alpha\zeta - \beta\eta) + a_{1,m}\lambda\mu}{\alpha\delta - \beta\gamma}. \end{aligned} \tag{3}$$

Whereby we have used the following abbreviations:

$$\begin{aligned} \alpha &= H'_m(k_2R_1)J_m(k_1R_1)k_1 - J'_m(k_1R_1)H_m(k_2R_1)k_2, \\ \beta &= J'_m(k_2R_1)J_m(k_1R_1)k_1 - J'_m(k_1R_1)J_m(k_2R_1)k_2, \\ \gamma &= H'_m(k_3R_2)H_m(k_2R_2)k_2 - H'_m(k_2R_2)H_m(k_3R_2)k_3, \\ \delta &= H'_m(k_3R_2)J_m(k_2R_2)k_2 - J'_m(k_2R_2)H_m(k_3R_2)k_3, \\ \epsilon &= H'_m(k_2R_1)J_m(k_2R_1)k_2 - J'_m(k_2R_1)H_m(k_2R_1)k_2, \\ \zeta &= J'_m(k_3R_2)J_m(k_2R_2)k_2 - J'_m(k_2R_2)J_m(k_3R_2)k_3, \\ \eta &= J'_m(k_3R_2)H_m(k_2R_2)k_2 - H'_m(k_2R_2)J_m(k_3R_2)k_3, \\ \kappa &= J'_m(k_3R_2)H_m(k_3R_2)k_3 - H'_m(k_3R_2)J_m(k_3R_2)k_3, \\ \lambda &= J'_m(k_1R_1)H_m(k_1R_1)k_1 - H'_m(k_1R_1)J_m(k_1R_1)k_1, \\ \mu &= H'_m(k_2R_2)J_m(k_2R_2)k_2 - J'_m(k_2R_2)H_m(k_2R_2)k_2, \\ \nu &= J'_m(k_2R_1)H_m(k_1R_1)k_1 - H'_m(k_1R_1)J_m(k_2R_1)k_2, \text{ and} \\ \sigma &= H'_m(k_1R_1)H_m(k_2R_1)k_2 - H'_m(k_2R_1)H_m(k_1R_1)k_1. \end{aligned} \tag{4}$$

For TE polarization one obtains analogously

$$\begin{aligned} B_{1,m} &= \frac{-B_{3,m}\tilde{\epsilon}\tilde{\kappa} + b_{1,m}(\tilde{\gamma}\tilde{\nu} + \tilde{\delta}\tilde{\sigma})}{\tilde{\alpha}\tilde{\delta} - \tilde{\beta}\tilde{\gamma}}, b_{2,m} = \frac{B_{3,m}\tilde{\beta}\tilde{\kappa} - b_{1,m}\tilde{\delta}\tilde{\lambda}}{\tilde{\alpha}\tilde{\delta} - \tilde{\beta}\tilde{\gamma}}, \\ B_{2,m} &= \frac{-B_{3,m}\tilde{\alpha}\tilde{\kappa} + b_{1,m}\tilde{\gamma}\tilde{\lambda}}{\tilde{\alpha}\tilde{\delta} - \tilde{\beta}\tilde{\gamma}}, \text{ and } b_{3,m} = -\frac{B_{3,m}(\tilde{\alpha}\tilde{\zeta} - \tilde{\beta}\tilde{\eta}) + b_{1,m}\tilde{\lambda}\tilde{\mu}}{\tilde{\alpha}\tilde{\delta} - \tilde{\beta}\tilde{\gamma}}. \end{aligned} \tag{5}$$

The abbreviated expressions $\tilde{\alpha}, \ldots, \tilde{\sigma}$ have the same structure as in case of TM polarization, except that the derived and the non-derived quantities are interchanged.

Excitation by a plane wave

The expansion coefficients of an incoming plane wave travelling along the positive x-directiong are given by [1]

$$A_{3,m} = E_{0,y}e^{\frac{\imath\pi}{4}m} \text{ and } B_{3,m} = E_{0,z}e^{\frac{\imath\pi}{4}m} \tag{6}$$

for TM and TE polarization, respectively. In the core region the regularity of the fields furthermore requires $a_{1,m} = b_{1,m} = 0$. With the known excitation coefficients it is straight forward to determine the remaining coefficients within the core and the shell region with the help of Eqs. (3) to (5). The fields in all domains can then be calculated from Eq. (1). By integration of the normal component of the Poynting vector along a closed path in the xy-plane within the exterior domain the absorbed and the scattered power per cylinder length can be determined:

$$\begin{aligned} P_{\mathrm{abs}} &= -\oint_{\Gamma} \frac{1}{2}\mathrm{Re}\{(\mathbf{E}_{\mathrm{s}} + \mathbf{E}_{\mathrm{i}}) \times (\mathbf{H}_{\mathrm{s}} + \mathbf{H}_{\mathrm{i}})^{*}\} \cdot \mathbf{n}\mathrm{d}s = P_{ext} - P_{sca}, \\ P_{\mathrm{sca}} &= \oint_{\Gamma} \frac{1}{2}\mathrm{Re}\{\mathbf{E}_{\mathrm{s}} \times \mathbf{H}_{\mathrm{s}}^{*}\} \cdot \mathbf{n}\mathrm{d}s, \text{ and} \\ P_{\mathrm{ext}} &= -\oint_{\Gamma} \frac{1}{2}\mathrm{Re}\{\mathbf{E}_{\mathrm{s}} \times \mathbf{H}_{\mathrm{i}}^{*} + \mathbf{E}_{\mathrm{i}} \times \mathbf{H}_{\mathrm{s}}^{*}\} \cdot \mathbf{n}\mathrm{d}s \end{aligned} \tag{7}$$

with

$$\begin{aligned} \mathbf{E}_{\mathrm{i}} &= \sum_{m=-\infty}^{\infty} \left(\iota A_{3,m}\mathbf{M}_{3,m} + B_{3,m}\mathbf{N}_{3,m}\right), \\ \mathbf{H}_{\mathrm{i}} &= \frac{n_3}{\iota Z_0} \sum_{m=-\infty}^{\infty} \left(\iota A_{3,m}\mathbf{N}_{3,m} + B_{3,m}\mathbf{M}_{3,m}\right), \end{aligned} \tag{8}$$

$$\begin{aligned} \mathbf{E}_{\mathrm{s}} &= \sum_{m=-\infty}^{\infty} \left(\iota a_{3,m}\mathbf{m}_{3,m} + b_{3,m}\mathbf{n}_{3,m}\right), \\ \mathbf{H}_{\mathrm{s}} &= \frac{n_3}{\iota Z_0} \sum_{m=-\infty}^{\infty} \left(\iota a_{3,m}\mathbf{n}_{3,m} + b_{3,m}\mathbf{m}_{3,m}\right). \end{aligned} \tag{9}$$

After performing the integration and division by the wire diameter and the incident intensity $I_{\mathrm{in}} = n_3|\mathbf{E}_0|^2/(2Z_0)$ one finally arrives at the dimensionless scattering, extinction absorption efficiencies

$$\begin{aligned} Q_{\mathrm{sca}}^{\mathrm{TM}} &= \frac{P_{\mathrm{sca}}^{\mathrm{TM}}}{2R_2 I_{\mathrm{in}}} = \frac{2}{k_3 R_2 \left|B_{3,0}\right|^2} \sum_{m=-\infty}^{\infty} \left|a_{3,m}\right|^2, \\ Q_{\mathrm{ext}}^{\mathrm{TM}} &= \frac{P_{\mathrm{ext}}^{\mathrm{TM}}}{2R_2 I_{\mathrm{in}}} = -\frac{2}{k_3 R_2 \left|A_{3,0}\right|^2} \sum_{m=-\infty}^{\infty} \mathrm{Re}\{a_{3,m}A_{3,m}^{*}\}, \\ Q_{\mathrm{abs}}^{\mathrm{TM}} &= Q_{\mathrm{ext}}^{\mathrm{TM}} - Q_{\mathrm{sca}}^{\mathrm{TM}}, \end{aligned} \tag{10}$$

For TM polarization and

$$\begin{aligned} Q_{\mathrm{sca}}^{\mathrm{TE}} &= \frac{P_{\mathrm{sca}}^{\mathrm{TE}}}{2R_2 I_{\mathrm{in}}} = \frac{2}{k_3 R_2 \left|A_{3,0}\right|^2} \sum_{m=-\infty}^{\infty} \left|b_{3,m}\right|^2, \\ Q_{\mathrm{ext}}^{\mathrm{TE}} &= \frac{P_{\mathrm{ext}}^{\mathrm{TE}}}{2R_2 I_{\mathrm{in}}} = -\frac{2}{k_3 R_2 \left|B_{3,0}\right|^2} \sum_{m=-\infty}^{\infty} \mathrm{Re}\{b_{3,m}B_{3,m}^{*}\}, \\ Q_{\mathrm{abs}}^{\mathrm{TE}} &= Q_{\mathrm{ext}}^{\mathrm{TE}} - Q_{\mathrm{sca}}^{\mathrm{TE}} \end{aligned} \tag{11}$$

for TE polarization.

Second harmonic generation

For the treatment of the second harmonic generation we assume that the fundamental wave is not depleted and the generated power of the second harmonic is much weaker than that of the fundamental. In this case the fundamental wave creates a nonlinear polarization in the nanowire core that drives the second harmonic emission; however the power loss of the fundamental wave as well as the interaction between the second harmonic and the fundamental can be neglected.

From the electric field of the fundamental wave within the $KNbO_3$ core we determine the driving nonlinear polarization at the second harmonic frequency. For a $KNbO_3$-crystal (point group mm2) with the c-axis aligned parallel to the nanowire axis (which is chosen to coincide with the z-direction of the coordinate system) the second harmonic component of the nonlinear polarization is given by [4,5]

$$\begin{pmatrix} P_x^{\mathrm{NL}}(2\omega) \\ P_y^{\mathrm{NL}}(2\omega) \\ P_z^{\mathrm{NL}}(2\omega) \end{pmatrix} = 2\varepsilon_0 \begin{pmatrix} 0 & 0 & 0 & 0 & d_{31} & 0 \\ 0 & 0 & 0 & d_{32} & 0 & 0 \\ d_{31} & d_{32} & d_{33} & 0 & 0 & 0 \end{pmatrix} \begin{pmatrix} E_x\,(\omega)^2 \\ E_y\,(\omega)^2 \\ E_z\,(\omega)^2 \\ 2E_y(\omega)E_z(\omega) \\ 2E_x(\omega)E_z(\omega) \\ 2E_x(\omega)E_y(\omega) \end{pmatrix}. \tag{12}$$

The nonlinear coefficients d_{ij} of $KNbO_3$ can be found in [5]. With the known nonlinear polarization we have to solve Maxwell's equations with a source current distribution at the second harmonic angular frequency 2ω:

$$\nabla \times \mathbf{E}(2\omega) = \imath 2\omega\mu_0 \mathbf{H}(\omega_{\mathrm{SHG}}), \tag{13}$$

$$\nabla \times \mathbf{H}(2\omega) = \mathbf{J}^{\mathrm{NL}} - \imath 2\omega\varepsilon_0\varepsilon\mathbf{E}(2\omega), \tag{14}$$

$$\mathbf{j}^{\mathrm{NL}}(2\omega) = -\imath 2\omega\mathbf{P}^{\mathrm{NL}}(2\omega).$$

This can either be done numerically or analytically by the same cylindrical harmonics expansion method we discussed for the fundamental excitation. The emission from a source inside the core is already included in Eq. (3) and (5). All that remains is the determination of the coefficients $a_{1,m}$ and $b_{1,m}$ for the given nonlinear polarization. As we are not interested in the correct field distribution within the whole core but only at the interface to the shell layer, we can perform a multipole expansion of the source current distribution.

The vector potential which is generated by a two dimensional current distribution in a homogeneous medium is given by [6]

$$\mathbf{A}(\mathbf{r}) = \mu_0 \frac{\imath}{4} \iint \mathbf{j}^{NL}(\mathbf{r}') H_0\,(k|\mathbf{r}-\mathbf{r}'|)\mathrm{d}x'\mathrm{d}y'. \tag{15}$$

The resulting magnetic field can be obtained by taking the curl of **A**:

$$\mathbf{H} = \frac{1}{\mu_0}\nabla \times \mathbf{A}. \tag{16}$$

Outside the source domain we can use Graf's formula [7] to express the Green's function $H_0\ (k|\mathbf{r}-\mathbf{r}'|)$ in terms of Bessel and Hankel functions of higher order centered at the origin:

$$H_0\ (k|\mathbf{r}-\mathbf{r}'|) = \sum_{m=-\infty}^{\infty} H_m(kr)e^{\imath m\phi}J_m(kr')e^{-\imath m\phi'}. \tag{17}$$

Thus outside of the current distribution the vector potential takes the form

$$\mathbf{A}(\mathbf{r}) = \mu_0 \sum_{m=-\infty}^{\infty} H_m(kr)e^{\imath m\phi}\mathbf{Q}^m \tag{18}$$

$$\text{with } \mathbf{Q}^m = \frac{\imath}{4}\iint \mathbf{j}^{NL}(\mathbf{r}')J_m(kr')e^{-\imath m\phi'}\,\mathrm{r}'\mathrm{d}r'\mathrm{d}\phi'. \tag{19}$$

By taking the curl of **A** and comparing the result with Eq. (1) we find that

$$a_{1,m} = \frac{k_1 Z_0}{n_1}\frac{1}{2}\left(Q_x^{m+1} + \imath Q_y^{m+1} + Q_x^{m-1} - \imath Q_y^{m-1}\ \right), \text{and} \tag{20}$$

$$b_{1,m} = \frac{k_1 Z_0}{n_1}\imath Q_z^m. \tag{21}$$

Once the coefficients of the source inside the core have been determined, the remaining expansion coefficients can be calculated by Eq. (3) and (5) without an externally incident field ($A_{3,m} = B_{3,m} = 0$). The emitted second harmonic power per wire length is then given by

$$P_{\mathrm{SHG}} = \frac{1}{2Z_0 k_3}\sum_{m=-\infty}^{\infty}\left(\left|a_{3,m}\right|^2 + \left|b_{3,m}\right|^2\right). \tag{22}$$

As in the undepleted pump approximation the emitted second harmonic power depends quadratically on the incident intensity, we will use the analogy with two photon excitation cross σ_{TPE} to quantize the second harmonic efficiency σ_{SHG}:

$$\sigma_{\mathrm{SHG}} = \frac{P_{\mathrm{SHG}}/(2\hbar\omega)}{[I_{\mathrm{in}}/(\hbar\omega)\,]^2} = \frac{\hbar\omega}{2}\frac{P_{\mathrm{SHG}}}{I_{\mathrm{in}}^2} \tag{23}$$

whereby $\hbar\omega$ is the photon energy of the fundamental wave and $I_{\mathrm{in}} = n_1|\mathbf{E}_0|^2/(2Z_0)$ is the incident intensity. As σ_{SHG} is usually very small, it is convenient to express it in units of Goeppert-Mayer per µm wire length:

$$1\,\frac{\mathrm{GM}}{\mu\mathrm{m}} = 10^{-58}\,\frac{\mathrm{s}\cdot\mathrm{m}^3}{\mathrm{photon}}\,\frac{\mathrm{m}}{\mu\mathrm{m}}. \tag{24}$$

Convergence and comparison with numerical results

In any practical implementation of the described algorithm the infinite sums in Eq. (1) have to be truncated at some finite expansion order $|m| \leq N$. We therefore investigated how many cylindrical harmonics have to retained in order to obtain accurate results. In all calculations we assumed a nanowire core made of $KNbO_3$ with a 7.5 nm thick gold shell illuminated with a TM polarized fundamental wave. The optical constants of $KNbO_3$ and gold were taken from references [5] and [8], respectively. For the exterior we assumed air ($n_3 = 1$). The calculation of the multipole coefficients of the nonlinear source current was performed by numerical integration of Eq. (19) in polar coordinates using the trapezoidal rule with a radial resolution of 1 nm and an angular step size of 1°.

The relative error of the emitted second harmonic power in dependence of the maximum expansion order of the fundamental wave N_{fun} and of the second harmonic N_{SHG} at a fundamental wavelength of 800 nm is shown in Fig. S2. The reference for the calculation of the relative error was obtained by increasing the expansion orders until the resulting change was smaller than the machine precision. As can be seen in Fig. S2 the proposed algorithm converges extremely fast. Even for a core radius as large as 200 nm only a few cylindrical harmonics need to be considered in order to achieve a good accuracy. However it is notable that, despite the much larger wavelength of the fundamental wave, at least as many expansion orders are required for the fundamental wave as for the second harmonic in order not to limit the overall convergence. This behavior is understandable as the nonlinear polarization depends quadratically on the fundamental fields and therefore any error in the fundamental wave will lead to twice the relative error in the second harmonic emission.

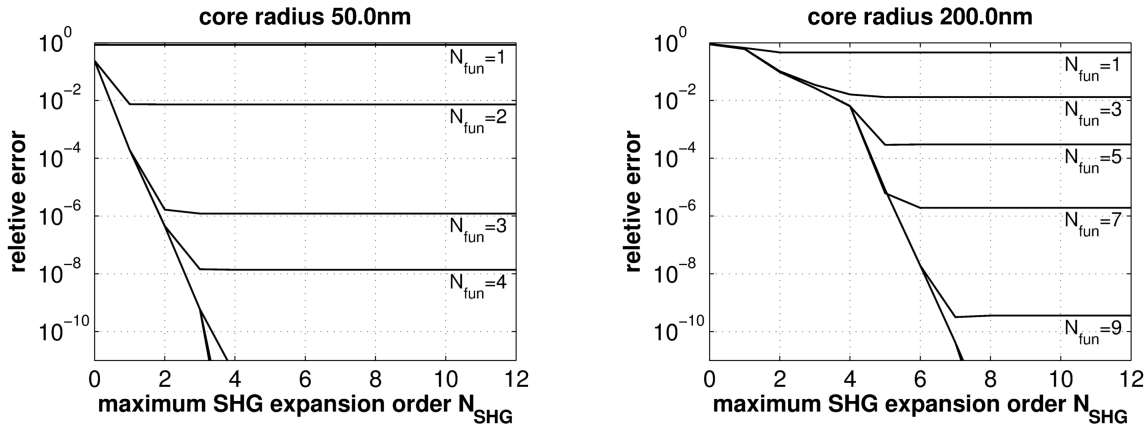

Figure S2: Convergence of the calculated SHG power with increasing order of the retained cylindrical harmonics for the expansion of the fundamental wave ($|m| \leq N_{\mathrm{fun}}$) and the second harmonic ($|m| \leq N_{\mathrm{SHG}}$). The fundamental wavelength was 800 nm.

To demonstrate the validity of the multipole expansion of the second harmonic source current we calculated the emitted second harmonic power of the real current distribution numerically with the finite differences frequency domain (FDFD) method [9]. A comparison between numerically calculated two photon excitation cross section and the results obtained by the cylindrical harmonics expansion is shown in Fig. S3 for various core radii with a 7.5nm thick gold shell. There is a perfect agreement between the results of the FDFD method and the analytical calculations. The deviation between both methods is less than 1%. This we assume is the accuracy limit of our FDFD implementation for the used grid resolution of 1.25 nm.

Furthermore we would like to point out that the FDFD method is about two orders of magnitude slower than the cylindrical harmonics expansion.

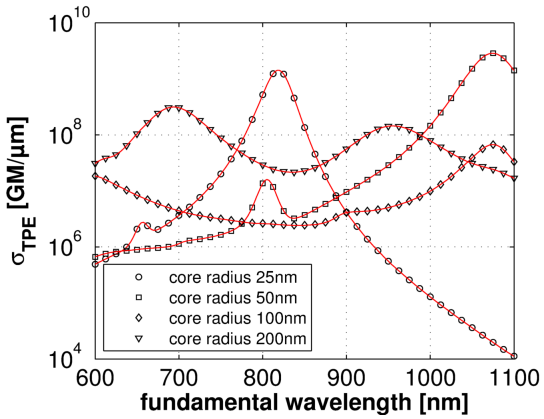

Figure S3: Comparison of the two photon excitation cross section calculated with the cylindrical harmonics expansion (symbols) with results obtained by numerical finite difference frequency domain calculations (solid lines).

3. Comparison of the plasmonic resonances of square and cylindrical nanowires

The emission of square nanowires cannot be treated by our analytical model as the field expansion relies on the circular symmetry. Nevertheless, linear calculations (Fig. S4) show that both the absorption cross-section and the field enhancement of a square wire are comparable to the cylindrical case.

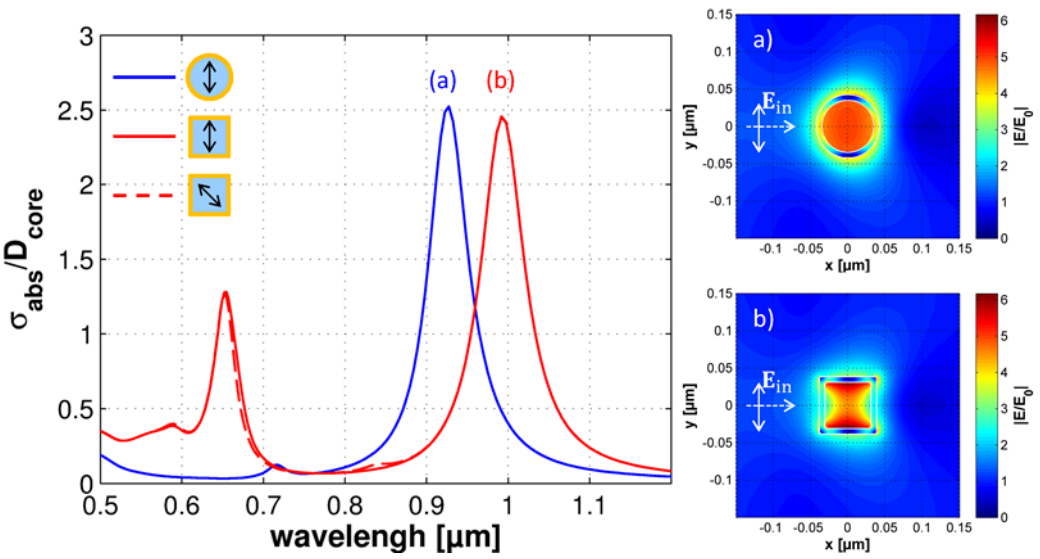

Figure S4:Comparison of the plasmonic resonances of square and cylindrical nanowires with equal core volume and shell thickness

4. Typical SHG images taken with the EMCCD

We measured the SHG signal with an EMCDD taking images (Fig. S5) at each different wavelength that are subsequently integrated to obtain the Fig. 5 a). Fig. S4 shows the SHG response of the uncoated nanowire and core-shell structure. A modulation of the SHG signal can be seen from the Fig. S5 (b) that can be attributed to several effects as cavity modes along the nanowires,[10] whispering gallery modes,[11] or hot spots due the an inhomogeneous gold shell. Such effects require further investigations to be clearly identified. They might also be a combination of several mechanisms.[12]

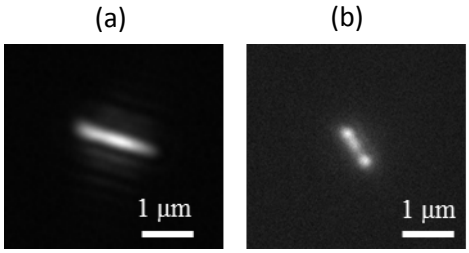

Figure S5: Measured SHG signal with the EMCCD after filtering out the near infrared excitation from (a) the bare nanowire and (b) the core-shell nanowire at 820 nm excitation wavelength.

References

1. C. F. Bohren and D. R. Huffman, *Absorption and Scattering of Light by Small Particles*, Wiley-VCH, Weinheim, 2004.
2. S.-C. Lee, *J. Quant. Spectrosc. Radiat. Transf.*, 1992, **48**, 119–130.
3. D. Wu, X. Liu, and B. Li, *J. Appl. Phys.*, 2011, **109**, 083540.
4. R. W. Boyd, *Nonlinear optics*, Amsterdam : Academic Press, 2nd editio., 2003.
5. V. G. Dmitriev, G. G. Gurzadyan, and D. N. Nikogosyan, *Handbook of Nonlinear Optical Crystals*, Springer, Berlin, 3rd edn., 1999, vol. 64.
6. J. D. Jackson, *Classical Electrodynamics*, Wiley, New York, 3rd edn., 1998.
7. M. Abramowitz and I. A. Stegun, Eds., *Handbook of Mathematical Functions*, United States Department of Commerce, Washington D.C., 10th edn., 1972, vol. 55.
8. P. B. Johnson and R. W. Christy, *Phys. Rev. E*, 1972, **6**, 4370–4379.
9. R. C. Rumpf, University of Central Florida, 2006.
10. R. Grange, G. Brönstrup, M. Kiometzis, A. Sergeyev, J. Richter, C. Leiterer, W. Fritzsche, C. Gutsche, A. Lysov, W. Prost, F.-J. Tegude, T. Pertsch, A. Tünnermann, and S. Christiansen, *Nano Lett.*, 2012, **12**, 5412–5417.
11. Y. Zhang, H. J. Zhou, S. W. Liu, Z. R. Tian, and M. Xiao, *Nano Lett.*, 2009, **9**, 2109–2112.
12. B. P. Mehl, R. L. House, A. Uppal, A. J. Reams, C. Zhang, J. R. Kirschbrown, and J. M. Papanikolas, *J. Phys. Chem. A*, 2010, **114**, 1241–1246.